nature physics

Article

https://doi.org/10.1038/s41567-024-02404-4

Superradiant and subradiant states in lifetime-limited organic molecules through laser-induced tuning

Received: 15 August 2023

Accepted: 19 January 2024

Published online: 19 February 2024



Christian M. Lange $m{0}^1$, Emma Daggett $m{0}^2$, Valentin Walther $m{0}^{1,2}$, Libai Huang $m{0}^2$ & Jonathan D. Hood $m{0}^{1,2} \boxtimes$

An array of radiatively coupled emitters provides a platform for generating, storing and manipulating quantum light. However, the simultaneous positioning and tuning of several lifetime-limited emitters into resonance remains a challenge. Here we report the creation of superradiant and subradiant entangled states in pairs of lifetime-limited and subwavelength-spaced organic molecules by permanently shifting them into resonance with laser-induced tuning. The molecules are embedded as defects in an organic nanocrystal. The pump light redistributes charges in the nanocrystal and dramatically increases the likelihood of resonant molecules. The frequency spectra, lifetimes and second-order correlation functions agree with a simple quantum model. This scalable tuning approach with organic molecules provides a pathway for observing collective quantum phenomena in subwavelength arrays of quantum emitters.

At subwavelength spacings, quantum emitters interact collectively with an electromagnetic field. Absorption and emission from separated atoms interfere, leading to super- and subradiant emitter states^{1,2}. The subradiant states form a decoherence-free subspace^{3,4} that is useful for manipulating quantum states⁵ and simulating many-body states^{6,7}. The collective emission also creates a wide variety of quantum states of $light^{8-10}$, which can be useful in quantum imaging and sensing 11 . In regular arrays, collective emitters can function as light-matter interfaces of unit coupling, thus allowing the efficient storage and manipulation of light^{4,12-15}. Although optical superradiance has been observed in a wide variety of atomic $^{16-20}$, solid-state $^{21-23}$ and molecular 24,25 emitters, the observation of individual superradiant and subradiant states has three major requirements: subwavelength positioning, tuning into resonance and minimizing dephasing from the environment. The realization of all three has only recently been demonstrated for two emitters using quantum dots coupled to a waveguide²⁶ and organic molecules tuned by nano-electrodes²⁷, but the challenge remains to scale this up to large system sizes.

In this work, we demonstrate a new scalable method for tuning lifetime-limited organic molecules in close proximity into resonance.

We observe superradiant and subradiant states for pairs of molecules separated by tens of nanometres as they are brought into resonance using laser-induced tuning. Dibenzoterrylene (DBT) molecules embedded as defects in an anthracene crystal ^{28,29} are excellent quantum emitters and lifetime-limited below 3 K (refs. 30,31). As first demonstrated in ref. 32, intense laser light tunes molecular resonances through the creation of excitons that Stark-shift molecules. In this work, we show that long exposure to laser light can permanently bring pairs of molecules spaced by tens of nanometres into resonance. This local decrease in inhomogeneous broadening indicates that some environmental variation can be decreased through laser-induced charge mobilization. The total inhomogeneous broadening of the system is not seen to decrease, suggesting that the charge mobilization increases the correlation length of environmental noise without uniformizing the entire host matrix.

We characterize several molecule pairs at large detuning and near resonance and find excellent agreement of the linewidths, lifetimes and second-order correlation functions with a simulation of a master equation. The agreement with a simple model, ease of fabrication and scalability of the tuning method demonstrate that organic

¹Department of Physics and Astronomy, Purdue University, West Lafayette, IN, USA. ²Department of Chemistry, Purdue University, West Lafayette, IN, USA. ⊠e-mail: hoodjd@purdue.edu

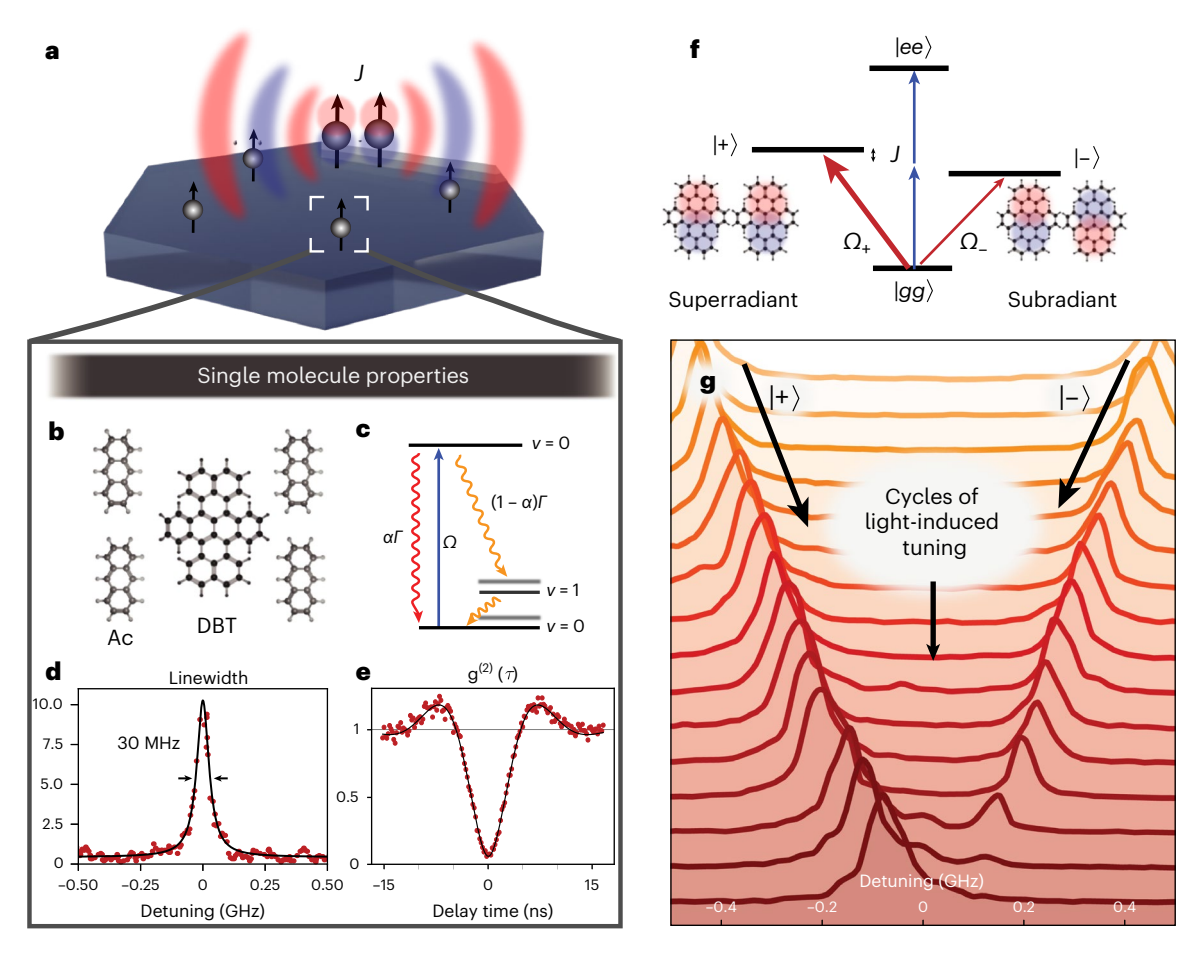


Fig. 1| **Overview of DBT interactions. a**, Two DBT molecules in an anthracene crystal (Ac) interact through their dipole moments with rate f. **b**, The DBT molecule is embedded as a defect into an anthracene crystal and has an electronic transition near 785 nm with a linear dipole moment. **c**, Level structure of DBT. The excited state decays with rate $\alpha\Gamma$ to the electronic and vibrational ground state, where α is the DWFC factor. The excited state also decays with rate $(1-\alpha)\Gamma$ to higher vibrational states and their phonon sidebands. The decay into

the ground vibrational state is filtered out, and the decay to the vibrational levels is used for all fluorescence measurements. \mathbf{d} , Lifetime-limited linewidth scan of a single DBT molecule at 2.7 K. \mathbf{e} , The $g^{(2)}(r)$ for a single molecule with $g^{(2)}(0)=0.065(9)$. \mathbf{f} , This interaction leads to collective superradiant $|+\rangle$ and subradiant $|-\rangle$ states. \mathbf{g} , Spectra of two molecules as they are tuned into resonance with intense illumination. The subradiant peak extinguishes as the detuning becomes smaller than the interaction J.

molecules are a promising platform for creating cooperative phenomena in arrays of quantum emitters. DBT molecules, as shown in Fig. 1a,b, are embedded as defects in anthracene nanocrystals^{28,29,33}, with a transition from the highest-occupied molecular orbital to the lowest-unoccupied molecular orbital near 785 nm (ref. 34). Each electronic state is accompanied by a manifold of vibrational states and phonon sidebands, as diagrammed in the level structure in Fig. 1c. Below 3 K, the linewidth of the electronic transition is lifetime-limited, as shown in Fig. 1d. The autocorrelation spectrum in Fig. 1e gives the likelihood of detecting two photons with a delay τ and shows a high purity of single-photon emission from a single molecule. The excited state decays to the zero-phonon line of the ground vibrational state with a probability of $\alpha = 30\%$, given by the product of the Debye-Waller and Franck-Condon (DWFC) factors, which are the fraction of emission into the zero-phonon line and the fraction of emission into the ground vibrational state, respectively. DBT and other polyaromatic hydrocarbons are leading candidates for solid-state quantum emitters and have demonstrated 94% indistinguishability for two photons from the same emitter³⁵, 70% indistinguishability for two photons from different emitters³⁶ and a photon collection efficiency of 99% (ref. 37).

Anthracene nanocrystals doped with a few hundred DBT molecules are self-assembled by precipitation from solution in a sonicator $^{\rm 33}$ and vary from 200 nm to 1 µm in size. The transition frequencies of a DBT molecule can be tuned by 100 GHz through exposure to intense laser light, as demonstrated in ref. 32. The tuning persists after the pump light is turned off and is probably due to a photoionization process in DBT, which results in an electron and hole pair with an extremely long recombination time. The charge and hole migrate apart and create an electric field that tunes the DBT molecule through a d.c. Stark shift. Because of the symmetry of the DBT/anthracene system, the Stark coupling is quadratic and the DBT molecule shifts only towards the red $^{\rm 44}$. Guest–host systems that lack centrosymmetry, such as DBT in 2,3-dibromonaphthalene, exhibit a large linear Stark effect $^{\rm 45}$.

We pump the nanocrystals with around 1 mW of 785 nm light focused through an objective to a waist of 1.5 μ m for tens of minutes. We then look for a two-photon peak with a height that depends on power squared, which indicates an interaction as described below. Out of 25 pumped nanocrystals, we observed ten signatures of interactions.

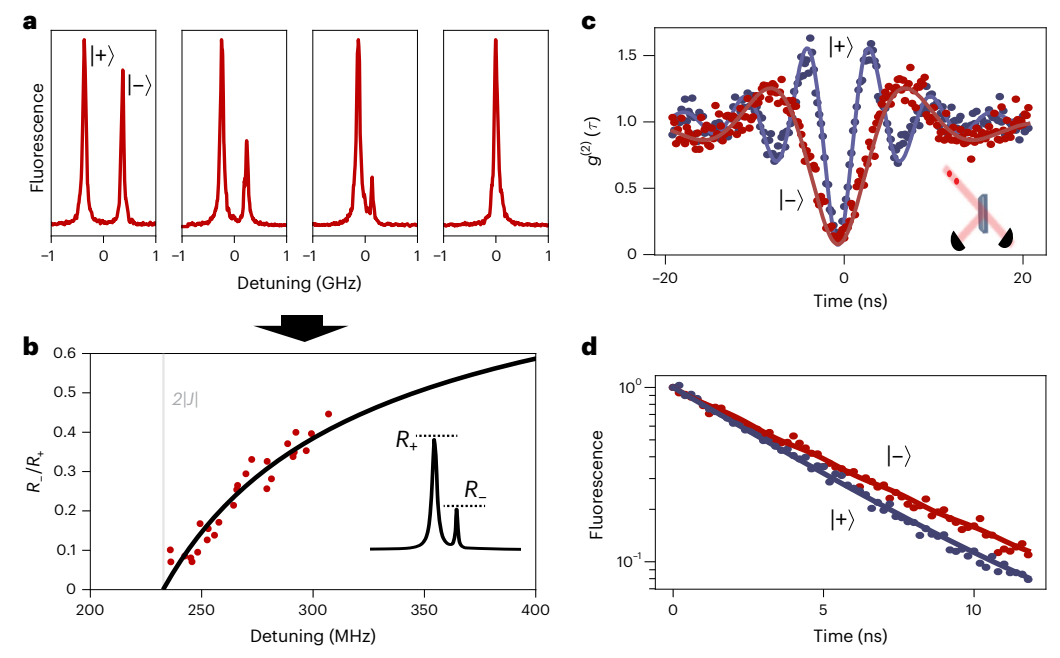


Fig. 2 | **Spectroscopy of two molecules tuned into resonance. a**, Spectra of the superradiant ($|+\rangle$) and subradiant ($|-\rangle$) states of two coupled molecules as the molecules are tuned into resonance. The tuning in **a** was done with 170 cycles of 100 s exposure to 4 kW cm⁻² of 785 nm laser light. **b**, Ratio of the heights of the subradiant and superradiant peaks as a function of detuning, fitted to a master equation simulation to obtain J=-116(15) MHz. The spectra were obtained at an excitation intensity of J=0.43 W cm⁻². **c,d** Second-order correlation functions

 $g^{(2)}(\tau)$ (**c**) and lifetimes (**d**) of a different pair of superradiant and subradiant peaks at $\Delta=2.6$ GHz detuning. The superradiant (subradiant) state has an increased (decreased) Rabi frequency, which results in faster (slower) oscillation of $g^{(2)}(\tau)$ for a given excitation power. The $g^{(2)}(\tau)$ functions are fitted to a master equation simulation to give J=1.0(1) GHz and $I/I_{\rm sat}=27(1)$, where $I_{\rm sat}$ is the saturation intensity of an uncoupled molecule. The lifetimes are fitted to give $I_0=33(1)$ MHz and $\alpha=0.11(3)$.

The molecules interact through the electric fields of their oscillating dipole moments. The dipole moments are linear and all aligned to the crystalline lattice 34 . The Hamiltonian for a system of N interacting dipoles in the rotating frame of the laser is

$$H = \sum_{i}^{N} \left(\delta_{i} - i \frac{\Gamma}{2} \right) \sigma_{i}^{\dagger} \sigma_{i} + \sum_{i \neq j}^{N} \left(J_{ij} - i \frac{\Gamma_{ij}}{2} \right) \sigma_{i}^{\dagger} \sigma_{j}, \tag{1}$$

where $\delta_i = \omega_i - \omega_L$ is the detuning from the laser frequency ω_L . The non-Hermitian rates Γ and Γ_{ij} are the spontaneous decay and dipole–dipole stimulated decay rates². The coherent dipole–dipole interaction J_{ij} generates energy exchange between molecules. In the near field, it is given by

$$J_{ij} = \frac{1}{4\pi\epsilon_0 \epsilon_r} \frac{\mathbf{d}_i \cdot \mathbf{d}_j - 3(\mathbf{d}_i \cdot \hat{\mathbf{r}})(\mathbf{d}_j \cdot \hat{\mathbf{r}})}{r^3}.$$
 (2)

As shown in the level structure in Fig. 1f, the singly excited states $|eg\rangle$ and $|ge\rangle$ are coupled by J to form a collective system. For molecules separated by a detuning of Δ , the eigenstates are $|+\rangle = \sin\theta \ |eg\rangle + \cos\theta \ |ge\rangle$ and $|-\rangle = \cos\theta \ |eg\rangle - \sin\theta \ |ge\rangle$ with energies $\pm \tilde{\Delta}/2 = \sqrt{\Delta^2/4 + J^2}$ (see Supplementary Information for details). Here, $\tan\theta = (2J)/(\Delta + \tilde{\Delta})$.

As the pumping laser shifts the molecules into resonance, the eigenstates become $% \left\{ 1,2,\ldots ,n\right\}$

$$|\pm\rangle = (|eg\rangle \pm |ge\rangle)/\sqrt{2}.$$
 (3)

In the limit of purely symmetric and antisymmetric states, the molecules are maximally entangled and share a single excitation before the system decays. Because the spacing of interacting molecules is much less than the excitation wavelength, they are each driven by the same Rabi frequency through the symmetric Hamiltonian $H_{\rm D} = \sum_i \frac{\Omega_{\rm R}}{2} \left(\sigma_i + \sigma_i^\dagger\right)$.

Figure 1g shows two interacting molecules tuning into resonance as they are pumped with intense laser light. As the detuning of the two molecules Δ becomes smaller than the interaction strength J, the antisymmetric subradiant state $|-\rangle$ goes dark to the symmetric drive. As shown in Fig. 2a,b, the splitting of the eigenstates converges to 2J, allowing the interaction strength to be determined from the extinction curve.

After the extinction of the subradiant state, one pair of molecules remained resonant for over 24 h of continuous monitoring. Other pairs of interacting molecules remained detuned by a few gigahertz despite undergoing tens of gigahertz of accumulated frequency shifting.

Figure 2c,d shows the $g^{(2)}(\tau)$ functions and lifetimes of a second pair of molecules with detuning $\Delta=2.6$ GHz. The $g^{(2)}(\tau)$ function measures the likelihood of detecting two photons at a time delay of τ . Above saturation, $g^{(2)}(\tau)$ exhibits Rabi oscillations that represent coherent population transfer between the ground and excited states. Driving at $I/I_{\rm sat}=27(1)$, we extracted $\Omega_+=3.8\Gamma$ and $\Omega_-=2.2\Gamma$ by fitting to an analytical expression for the $g^{(2)}(\tau)$ of a two-state system⁴⁶. The measured lifetimes were $\tau_+=4.3(1)$ ns and $\tau_-=5.2(2)$ ns, whereas a non-interacting molecule typically has a lifetime of $\tau=4.5$ ns.

The Rabi frequency exhibits a more pronounced effect because it is related only to the transition frequency with which the molecules interact. The lifetime, in contrast, contains both the decay from the interacting transition and the decay to the other vibrational states and phonon sidebands.

Figure 3a shows a series of fluorescence spectra of two interacting molecules with increasing excitation power. At high excitation power, the doubly excited state $|ee\rangle$ is populated and a two-photon peak emerges in the centre of the coupled resonances. As derived in the Supplementary Information, the two-photon peak scales as $\frac{\Omega^4 J^2}{\Gamma^2 \Delta^4}$ in the limit of large detuning. Driving near the two-photon resonance can generate squeezed light⁴⁷ or entangle non-resonant states⁴⁸. Figure 3b,c compares these spectra with a master equation simulation

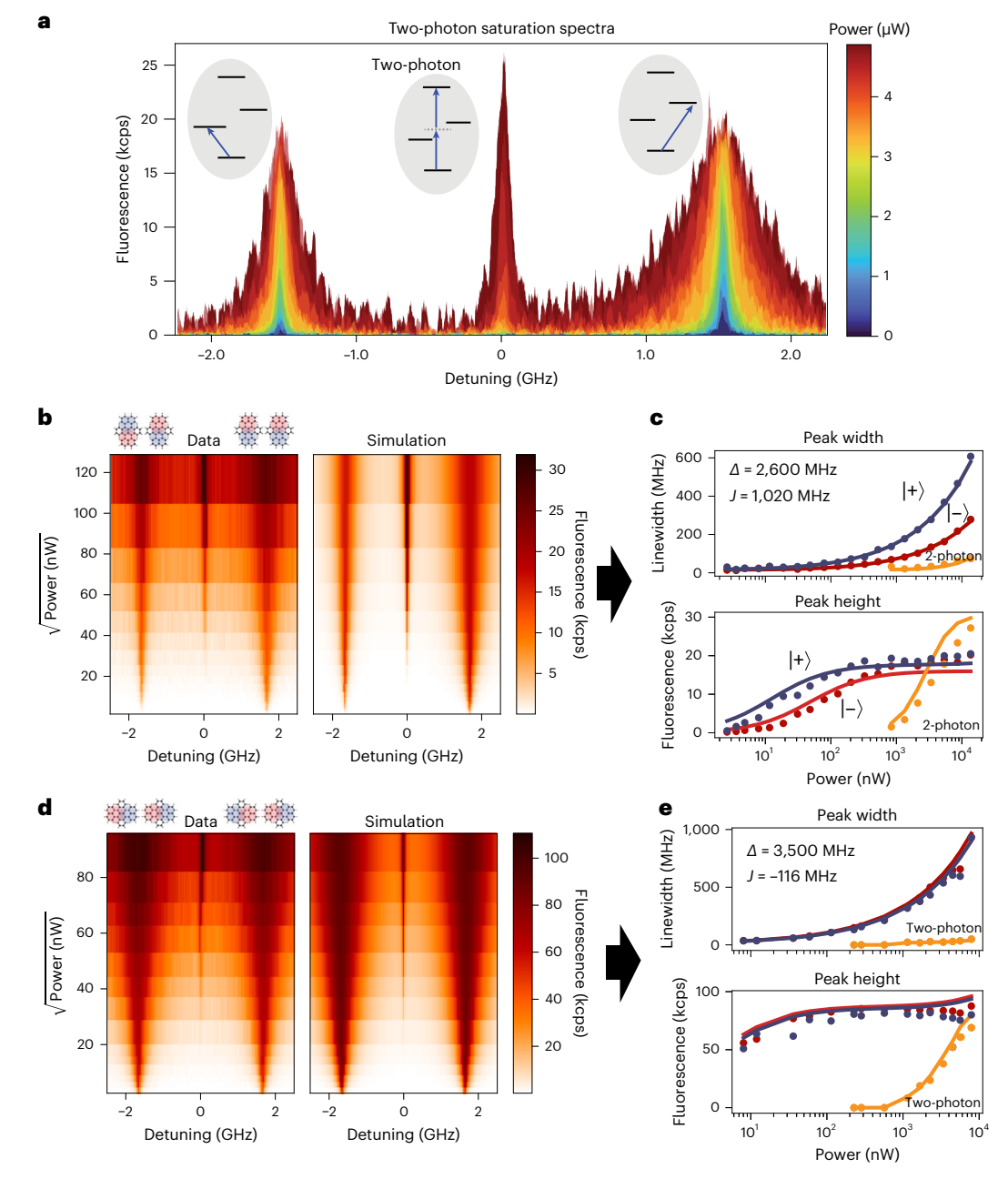


Fig. 3 | **Simulation of saturation spectra. a**, Saturation spectra for molecules in the H aggregate orientation, where the dipoles are oriented perpendicular to the separation vector and the superradiant state is higher in energy than the subradiant. The spectra are aligned by the average of their superradiant and subradiant frequencies. **b**, The spectra in **a** are stacked to illustrate the appearance of the two-photon peak as the excitation power increases. **c**, The heights and widths of the spectra in **b** are extracted with Lorentzian fits and compared with a master equation simulation. The simulation parameters are $\Gamma = 33(1) \, \text{MHz}, J = 1.0(1) \, \text{GHz}$ and $\alpha = 0.11(3)$, which are fitted through $g^{(2)}(\tau)$ and

lifetime simulations. **d**, Saturation spectra for molecules in the J aggregate orientation, where the dipoles are oriented parallel to the separation vector and the superradiant state is lower in energy than the subradiant. **e**, The heights and widths of the spectra in **d** are extracted with Lorentzian fits and compared with a master equation simulation. The simulation parameters are $\Gamma = 37(2)$ MHz, J = -116(15) MHz and $\alpha = 0.135(30)$. The dephasing rates for all simulations are 10(5) MHz, which are obtained by comparing the zero-power linewidths and lifetimes.

with J = 1.0(1) GHz, a DWFC factor $\alpha = 0.11(3)$, 10(5) MHz dephasing and $\Gamma = 33(1)$ MHz.

The values of Γ , α and J were extracted by simultaneously fitting the master equation simulation to the $g^{(2)}(\tau)$ and decay curves shown in Fig. 2c,d. The frequency of the Rabi oscillations in the $g^{(2)}(\tau)$ functions are more sensitive to J, whereas the lifetimes are more sensitive to α and Γ . The dephasing was estimated by comparing the lifetimes of the states with their linewidths in the far-detuning limit, where the molecules are approximately uncoupled. The fitting procedure is described in more detail in the Supplementary Information.

To illustrate the agreement between experiment and theory, the scattering rates and linewidths of the three peaks are extracted with Lorentzian fits and plotted against the simulation values in Fig. 3c. Above saturation, the asymmetry of the superradiant and subradiant peaks depends on J and α . In contrast, the height of the two-photon peak is sensitive to J and the dephasing, whereas the saturated linewidths are primarily sensitive to J. Because the superradiant state is higher in energy than the subradiant, we can infer that the molecules are in the H aggregate orientation, with dipoles roughly perpendicular to the separation vector. Figure 3d,e shows a similar set of data for a

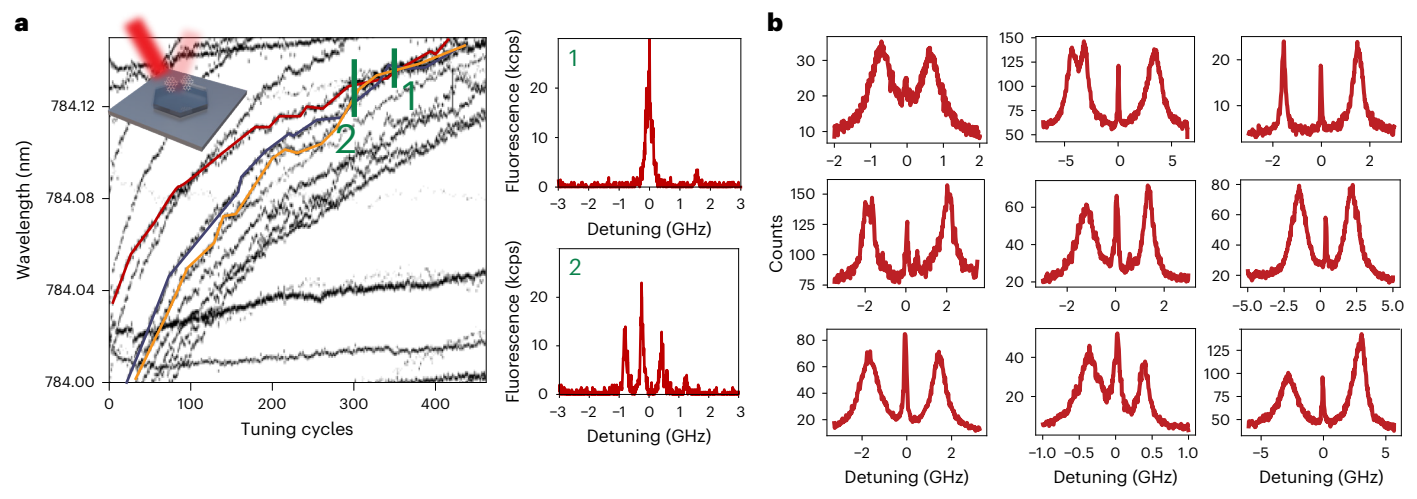


Fig. 4 | **Laser-induced tuning. a**, Tuning many molecules in a single nanocrystal. The nanocrystal is pumped with 16 kW cm^{-2} for 10 s between probes. Panels (1) and (2) show three resonances being tuned within a single linewidth. **b**, Nine two-photon peaks from separate nanocrystals, each pumped with 10 mW of light

for 30 min. The coupled molecules exhibit both H aggregate and J aggregate orientations, as well as weak- and strong-interaction strength regimes. Several of the spectra indicate that there are more than two interacting molecules.

pair of molecules in the Jaggregate orientation, with J=-116(15) MHz, $\alpha=0.135(30)$ and $\Gamma=37(2)$ MHz, which are extracted from lifetime measurements and the extinction curve in Fig. 2b. An approximate dephasing rate of 10(5) MHz for both pairs of molecules is estimated by comparing the zero-power linewidths with the lifetimes. For both pairs of molecules, the extracted values of J, α and Γ are consistent with measurements at several detunings. Because J is sensitive to the separation of the dipoles, this is evidence that the tuning mechanism is not accompanied by the movement of the molecules to different positions in the lattice or to the formation of aggregates, as J would be orders larger 25 . The DWFC factors of $\alpha=0.135(30)$ and 0.11(3) are lower than the reported value of 0.3 for a single DBT molecule. This may be due to the close proximity of the molecules, differences in the synthesis or misalignment of the dipoles.

Figure 4a shows many molecules in a single nanocrystal shifting during successive pump cycles. The coloured lines highlight three molecules being brought into resonance from a detuning of over 25 GHz, with spectra of the three molecules before and after shown to the right. After laser-induced shifting, ten nanocrystals out of 25 had clear two-photon peaks. Figure 4b shows several examples of interacting molecules, each from a different nanocrystal. Interestingly, the coupled molecules commonly came into resonance with additional molecules, and some remained in resonance even during tuning. For example, the subradiant peak in the lower right spectrum of Fig. 4b is broader than the corresponding superradiant peak because it overlaps an additional resonance, as verified by the $g^{(2)}(\tau)$ and saturation spectra. This result is promising for the creation of many-body interactions and will be the subject of future research. The length scale over which inhomogeneous broadening can be reduced is probably determined by the length scale of imperfections in the lattice, which cause inhomogeneous broadening. With an increase in the purity of nanocrystal synthesis or dopant density of high-purity synthesis methods like cosublimation, the length scale of this effect could be increased, allowing for the creation of many-body collective effects in the solid state.

Conclusion

This work is a demonstration of permanently tuning lifetime-limited solid-state emitters into resonance and preparing superradiant and subradiant states. Laser-induced tuning increases the likelihood of obtaining resonant molecules within a nanocrystal, and two-photon peaks from interacting molecules are observed in a third of the

nanocrystals. We characterized interacting molecules in different orientations, extracted the interaction strengths and branching ratios, and showed good agreement with a simple theory.

This light-based tuning method can be scaled to larger arrays of emitters through several routes. Increasing the doping or decreasing the inhomogeneous broadening will increase the number of interacting molecules. Larger crystals have been co-sublimated with two orders of magnitude smaller inhomogeneous broadening³⁸. If molecules could be individually targeted³², such as through superresolution techniques or scanning near-field optical microscopy, then creating a two-dimensional array of resonant emitters with subwavelength spacing may be possible. Organic molecules have also been shown to be compatible with nanophotonic devices³⁹, which would enhance the combined Debye–Waller/Franck–Condon factor, increase the photon collection efficiency and create long-range interactions.

Collective states of arrays of organic molecules have many applications. Superradiant light could measure phase or intensity with Heisenberg sensitivity⁴⁰, as the signal-to-noise ratio scales with the photon number, not its square root. The correlations between the emitters could be engineered to create many-photon quantum light⁴¹, for example, cluster states for one-way quantum computation or entangled states that are more robust against photon loss. The entangled states of molecules embedded in a lattice also have fundamental interests, for example, elucidating the role of dephasing and vibrational states in collective states^{42,43}. By demonstrating the ability to tune and characterize entanglement in a system with disorder and decoherence processes, this study could lead to a better understanding of coherence phenomena in molecular aggregates and other solid-state collective systems.

Online content

Any methods, additional references, Nature Portfolio reporting summaries, source data, extended data, supplementary information, acknowledgements, peer review information; details of author contributions and competing interests; and statements of data and code availability are available at $\frac{1}{1000} = \frac{1}{1000} = \frac{1}{1000}$

References

- Dicke, R. H. Coherence in spontaneous radiation processes. Phys. Rev. 93, 99–110 (1954).
- Reitz, M., Sommer, C. & Genes, C. Cooperative quantum phenomena in light–matter platforms. PRX Quantum 3, 010201 (2022).

- Lidar, D. A., Chuang, I. L. & Whaley, K. B. Decoherence-free subspaces for quantum computation. *Phys. Rev. Lett.* 81, 2594–2597 (1998).
- Facchinetti, G., Jenkins, S. D. & Ruostekoski, J. Storing light with subradiant correlations in arrays of atoms. *Phys. Rev. Lett.* 117, 243601 (2016).
- Beige, A., Braun, D. & Knight, P. L. Driving atoms into decoherencefree states. New J. Phys. 2, 22 (2000).
- Perczel, J. et al. Topological quantum optics in two-dimensional atomic arrays. Phys. Rev. Lett. 119, 023603 (2017).
- Parmee, C. D. & Ruostekoski, J. Signatures of optical phase transitions in superradiant and subradiant atomic arrays. Commun. Phys. 3, 205 (2020).
- Porras, D. & Cirac, J. I. Collective generation of quantum states of light by entangled atoms. *Phys. Rev. A* 78, 053816 (2008).
- González-Tudela, A., Paulisch, V., Chang, D. E., Kimble, H. J. & Cirac, J. I. Deterministic generation of arbitrary photonic states assisted by dissipation. *Phys. Rev. Lett.* 115, 163603 (2015).
- Holzinger, R., Plankensteiner, D., Ostermann, L. & Ritsch, H. Nanoscale coherent light source. *Phys. Rev. Lett.* 124, 253603 (2020).
- Berchera, I. R. & Degiovanni, I. P. Quantum imaging with sub-Poissonian light: challenges and perspectives in optical metrology. *Metrologia* 56, 024001 (2019).
- Bettles, R. J., Gardiner, S. A. & Adams, C. S. Enhanced optical cross section via collective coupling of atomic dipoles in a 2D array. Phys. Rev. Lett. 116, 103602 (2016).
- Asenjo-Garcia, A., Moreno-Cardoner, M., Albrecht, A., Kimble, H. J. & Chang, D. E. Exponential improvement in photon storage fidelities using subradiance and 'selective radiance' in atomic arrays. *Phys. Rev. X* 7, 031024 (2017).
- Rui, J. et al. A subradiant optical mirror formed by a single structured atomic layer. Nature 583, 369–374 (2020).
- Bekenstein, R. et al. Quantum metasurfaces with atom arrays. Nat. Phys. 16, 676–681 (2020).
- Eschner, J., Raab, C., Schmidt-Kaler, F. & Blatt, R. Light interference from single atoms and their mirror images. *Nature* 413, 495–498 (2001).
- 17. Goban, A. et al. Superradiance for atoms trapped along a photonic crystal waveguide. *Phys. Rev. Lett.* **115**, 063601 (2015).
- McGuyer, B. H. et al. Precise study of asymptotic physics with subradiant ultracold molecules. *Nat. Phys.* 11, 32–36 (2015).
- Solano, P., Barberis-Blostein, P., Fatemi, F. K., Orozco, L. A. & Rolston, S. L. Super-radiance reveals infinite-range dipole interactions through a nanofiber. *Nat. Commun.* 8, 1857 (2017).
- 20. Ferioli, G. et al. Laser-driven superradiant ensembles of two-level atoms near Dicke regime. *Phys. Rev. Lett.* **127**, 243602 (2021).
- Scheibner, M. et al. Superradiance of quantum dots. Nat. Phys. 3, 106–110 (2007).
- Sipahigil, A. et al. An integrated diamond nanophotonics platform for quantum-optical networks. Science 354, 847–850 (2016)
- Blach, D. D. et al. Superradiance and exciton delocalization in perovskite quantum dot superlattices. *Nano Lett.* 22, 7811–7818 (2022).
- Hettich, C. et al. Nanometer resolution and coherent optical dipole coupling of two individual molecules. Science 298, 385–389 (2002).
- Lim, S.-H., Bjorklund, T. G., Spano, F. C. & Bardeen, C. J. Exciton delocalization and superradiance in tetracene thin films and nanoaggregates. *Phys. Rev. Lett.* 92, 107402 (2004).
- Tiranov, A. et al. Collective super- and subradiant dynamics between distant optical quantum emitters. Science 379, 389–393 (2023).

- Trebbia, J.-B., Deplano, Q., Tamarat, P. & Lounis, B. Tailoring the superradiant and subradiant nature of two coherently coupled quantum emitters. *Nat. Commun.* 13, 2962 (2022).
- Tamarat, P., Maali, A., Lounis, B. & Orrit, M. Ten years of single-molecule spectroscopy. J. Phys. Chem. A 104, 1–16 (2000).
- 29. Toninelli, C. et al. Single organic molecules for photonic quantum technologies. *Nat. Mater.* **20**, 1615–1628 (2021).
- 30. Clear, C. et al. Phonon-induced optical dephasing in single organic molecules. *Phys. Rev. Lett.* **124**, 153602 (2020).
- 31. Wang, D. et al. Turning a molecule into a coherent two-level quantum system. *Nat. Phys.* **15**, 483–489 (2019).
- Colautti, M. et al. Laser-induced frequency tuning of Fourier-limited single-molecule emitters. ACS Nano 14, 13584–13592 (2020).
- Pazzagli, S. et al. Self-assembled nanocrystals of polycyclic aromatic hydrocarbons show photostable single-photon emission. ACS Nano 12, 4295–4303 (2018).
- Nicolet, A. A. L. et al. Single dibenzoterrylene molecules in an anthracene crystal: main insertion sites. *Chem. Phys. Chem.* 8, 1929–1936 (2007).
- Rezai, M., Wrachtrup, J. & Gerhardt, I. Coherence properties of molecular single photons for quantum networks. *Phys. Rev. X* 8, 031026 (2018).
- 36. Duquennoy, R. et al. Singular spectrum analysis of two-photon interference from distinct quantum emitters. *Phys. Rev. Res.* **5**, 023191 (2023).
- 37. Wrigge, G., Gerhardt, I., Hwang, J., Zumofen, G. & Sandoghdar, V. Efficient coupling of photons to a single molecule and the observation of its resonance fluorescence. *Nat. Phys.* **4**, 60–66 (2008).
- Ambrose, W. P., Basché, T. & Moerner, W. E. Detection and spectroscopy of single pentacene molecules in a p-terphenyl crystal by means of fluorescence excitation. J. Chem. Phys. 95, 7150–7163 (1991).
- 39. Rattenbacher, D. et al. Coherent coupling of single molecules to on-chip ring resonators. *New J. Phys.* **21**, 062002 (2019).
- Paulisch, V., Perarnau-Llobet, M., González-Tudela, A. & Cirac, J. I. Quantum metrology with one-dimensional superradiant photonic states. *Phys. Rev. A* 99, 043807 (2019).
- Tziperman, O. et al. Spontaneous emission from correlated emitters. Preprint at https://doi.org/10.48550/arXiv.2306.11348 (2023).
- 42. Gurlek, B., Sandoghdar, V. & Martin-Cano, D. Engineering long-lived vibrational states for an organic molecule. *Phys. Rev. Lett.* **127**, 123603 (2021).
- Zirkelbach, J. et al. High-resolution vibronic spectroscopy of a single molecule embedded in a crystal. J. Chem. Phys. 156, 104301 (2022).
- Schädler, K. G. et al. Electrical control of lifetime-limited quantum emitters using 2D materials. *Nano Lett.* 19, 3789–3795 (2019).
- Moradi, A., Ristanović, Z., Orrit, M., Deperasińska, I. & Kozankiewicz, B. Matrix-induced linear Stark effect of single dibenzoterrylene molecules in 2,3-dibromonaphthalene crystal. Chem. Phys. Chem 20, 55–61 (2019).
- Grandi, S. et al. Quantum dynamics of a driven two-level molecule with variable dephasing. *Phys. Rev. A* 94, 063839 (2016).
- 47. Martín-Cano, D., Haakh, H. R., Murr, K. & Agio, M. Large suppression of quantum fluctuations of light from a single emitter by an optical nanostructure. *Phys. Rev. Lett.* **113**, 263605 (2014).
- Vivas-Viaña, A., Martín-Cano, D. & Muñoz, C. S. Dissipative stabilization of maximal entanglement between non-identical emitters via two-photon excitation. Preprint at https://arxiv.org/ abs/2306.06028 (2023).

Publisher's note Springer Nature remains neutral with regard to jurisdictional claims in published maps and institutional affiliations.

Springer Nature or its licensor (e.g. a society or other partner) holds exclusive rights to this article under a publishing agreement with

the author(s) or other rightsholder(s); author self-archiving of the accepted manuscript version of this article is solely governed by the terms of such publishing agreement and applicable law.

@ The Author(s), under exclusive licence to Springer Nature Limited 2024

Data availability

All data supporting this study are available from figshare at https://doi.org/10.6084/m9.figshare.24969456. Source data are provided with this paper.

Code availability

The simulation code is available from figshare at https://doi.org/10.6084/m9.figshare.24969456.

Acknowledgements

J.H. and L.H. acknowledge support from the National Science Foundation (Grant No. DMREF-2324299) and the Office of Science of the US Department of Energy through the Quantum Science Center, a National Quantum Information Science Research Center. We thank C. Toninelli and A. Clark for nanocrystal synthesis and characterization advice.

Author contributions

J.H. and L.H. conceived the experiment. C.L. and J.H. designed the experiment, performed the numerical simulations and wrote the

paper. C.L. and E.D. collected the data. C.L., V.W. and J.H. performed the analytic calculations. All authors interpreted the results.

Competing interests

The authors declare no competing interests.

Additional information

Supplementary information The online version contains supplementary material available at https://doi.org/10.1038/s41567-024-024-04-4.

Correspondence and requests for materials should be addressed to Jonathan D. Hood.

Peer review information *Nature Physics* thanks the anonymous reviewer(s) for their contribution to the peer review of this work.

 $\label{lem:complex} \textbf{Reprints and permissions information} \ is \ available \ at \\ www.nature.com/reprints.$